Palaeoclimatic and Palaeoenvironmental history of the late Quaternary sediments from the Indian sector of Southern Ocean: Rock Magnetic and Geochemical Signals

M.C. Manoj[1], M. Thamban[1], N. Basavaiah[2] and Rahul Mohan[1]

[1] National Centre for Antarctic and Ocean Research, Headland Sada, Goa, India.

[2] Indian Institute of Geomagnetism, New Panvel (W), Mumbai, India.

Introduction

Southern Ocean was a key element in the evolution of the late Quaternary millennial climate changes and represents a junction box of global conveyor-belt circulation. Our study attempts to evaluate the different environmental magnetic and geochemical parameters as palaeoclimatic proxy indicators in a well-dated sediment record from the Indian sector of Southern Ocean and to correlate with the major environmental changes other global palaeoclimatic records during the late Quaternary.

Study Region

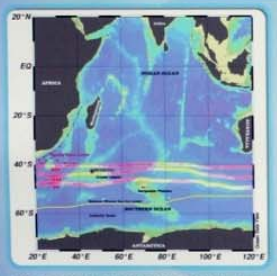

Fig. 1. Location map of the studied core

The Indian sector of the Southern Ocean is characterized by several circumpolar fronts.

Major fronts:-

- Subtropical Front (STF)
- Sub-Antarctic Front (SAF)
- Polar Front (PF)

Major water masses:-

- Antarctic Bottom Water (AABW)
- Circumpolar Deep Water (CDW)
- Antarctic Intermediate Water (AAIW)

Materials and Methods

A 7.54 m long sediment core (SK 200/22a) collected from the Indian sector of Southern Ocean, located at 43° 42'S and 45° 04'E, onboard *ORV Sagar Kanya* (SK 200), was used for this study.

Chronological control was obtained by accelerator mass spectrometry (AMS) radiocarbon (^{14}C) dates using two planktonic foraminifera species, *Globigerina bulloides* and *Neogloboquadrina pachyderma*. The radiocarbon ages were calibrated to calendar ages using Calib5.0.2 programme.

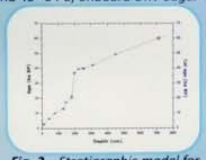

Fig. 2. Stratigraphic model for SK200/22a

Major proxy parameters studied in the core include:

- ✓ Environmental magnetic parameters using standard procedures.
- ✓ Inorganic element chemistry using ICPMS.
- ✓ Organic and inorganic carbon using TOC Analyser.
- ✓ The coarse fractions (>125μm) were studied for estimating the Ice Rafted Debris (IRD) content in the sediment.
- ✓ The stable isotope ($\delta^{18}O$ and $\delta^{13}C$) of *Neogloboquadrina pachyderma* tests using IRMS.

Results and Discussions

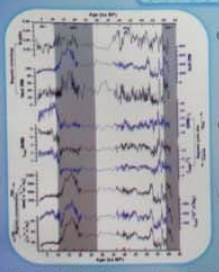

Fig. 3. Profile of the environmental magnetic parameters

- ***Magnetic Concentration*** - The last deglaciation shows a rapid increase in values of χ, χ_{ARM} and SIRM, with substantial increase between 18.5 and 13 kaBP.
- ***Magnetic grain size***- Fine grained magnetic minerals during MIS 1 and early MIS 3 suggest a reduced eroding capability of the currents.
- ***Magnetic mineralogy***- The high S-ratio and high Soft IRM values suggest that mineralogy is dominated by fine grained low-coercivity magnetite and titano-magnetite.

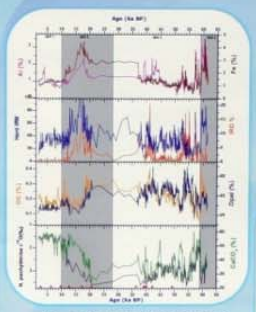

Fig. 4. Downcore variations of productivity and lithogenic proxies

- Geochemical proxies like Al and Fe, IRD and rock magnetic properties shows a substantial increase in lithogenic input between 18.5 and 13 ka BP (Fig. 4).
- Results showing high but variable opal, organic carbon and lithogenous fluxes during MIS 3 and LGM.

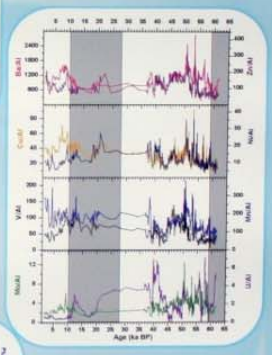

Fig. 5. Downcore variations of geochemical proxies

- The high Al normalized values of U, Mo, and V occur during glacial periods (MIS 2 and MIS 4) and certain intervals of MIS 3 reveals the existence of suboxic bottom waters.

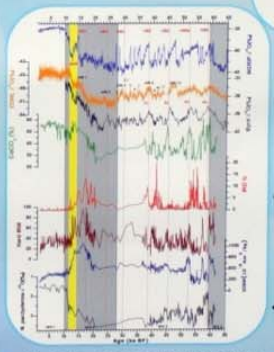

Fig. 6. Comparison of SK 200/22a with Antarctic and Greenland ice cores record.

- ❖ Comparison of the magnetic and geochemical proxies revealed that the lithogenic input fluctuated in tandem with sea surface warming and calcite productivity.
- ❖ Periods of enhanced lithogenic input and calcite productivity were synchronous with the millennial-scale Antarctic warming events, indicating an Antarctic linkage.
- ❖ Major IRD events are clearly out-of-phase with the northern hemisphere Heinrich events.

Conclusions

- ➢ The magnetic, $\delta^{18}O$ and $CaCO_3$ records suggest that past changes in sea surface warming, intensity of ACC, calcite content and lithogenic input were closely interlinked and responded to the climatic changes in the southern hemisphere.
- ➢ The ice rafted debris record revealed major ice rafting events during 13-20 kaBP, 23-30 kaBP, 40-44 kaBP and 52-58 kaBP with an out-of-phase relation with magnetic (lithogenic) and calcite productivity.
- ➢ The timing and characteristics of the multiple proxy record reported here clearly indicate an out-of-phase north-south linkage through the bipolar seesaw mechanism.

Acknowledgments

The authors are grateful to National Centre for Antarctic & Ocean Research (NCAOR), the Ministry of Earth Sciences (MoES), India and Indian National Science Academy (INSA) for providing with funds and supports.

INQUA International Union for Quaternary Research

E-mail: manojmc@ncaor.org

XVIII. INQUA BERN 2011 SWITZERLAND

Millennial-scale variations in East Asian summer monsoon during the last glacial period based on Mg/Ca and oxygen isotope of *Globigerinoides ruber* from the northern East China Sea

ID 2010
Isotope hydrology as a tracer of Quaternar climates

Yoshimi KUBOTA[1], Katsunori KIMOTO[2], Ryuji TADA[1], Masao UCHIDA[3], Ken IKEHARA[4]

1. University of Tokyo, Japan (yoshimi@eps.s.u-tokyo.ac.jp). 2. Japan Agency for Marine-Earth Science and Technology (JAMSTEC) , Japan. 3. National Institute for Environment Studies (NIES), Japan, 4. Geological Survey of Japan, National Institute of Advanced Industrial Science and Technology (AIST), Japan.

Questions

Does sea surface salinity in the northern East China Sea oscillate in harmony with Dansgaard-Oeschgar cycles during Marine Isotope Stage 3?

It has been suggested that changes in fresh water discharge from the Yellow and Yangtze Rivers attributed to deposition of dark and light layers in the Japan Sea, which are in association with Dansgaard-Oeschger (D-O) cycles [Tada et al., 1999]. This study aims to reconstruct sea surface salinity in the northern East China Sea in order to test this scenario.

East China Sea to Japan Sea

Temporal variation patterns of oscillations in grayscale (L*) of the hemipelagic sediments in the Japan sea are coincide with the D-O cycles in Greenland ice cores. The grayscale principally reflect organic carbon contents (C_{org}) that was controlled by primary production during the MIS3 [Tada et al., 1999]. Deposition of dark layers contain higher C_{org} , and were attributed to nutreint-rich and low-salinity water from the East China Sea.

Fig. 3 Photo of a sediment in the Japan Sea, water depth of 2074 m.

South China → Summer monsoon rainfall → **East China Sea** → Nutrient-rich & low-salinity coastal water → **Japan Sea** → High primary production → Organic matter → Dark layer

Oceanography

Summer at present

Surface salinity in the northen East China Sea
Discharge of the Yangtze River (Changjiang)
Rainfall in the catchment area of Yangtze River
[Delcroix and Murtugudde, 2002]

Fig. 1 Present current system in the East China Sea after Ichikawa and Beardsley [2002] and location of cores KR07-12.

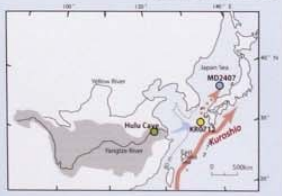

Fig. 2 Locations of the studied site (KR07-12), MD2407 in the Japan Sea [Kido et al.], and Hulu Cave [Wang et al., 2001]. Shaded zone represents the drainage area of the Yangtze River. 80 m sea-level drop corresponds MIS3.

Age model

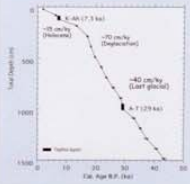

Fig. 4 A depth versus calendar age for core KR07-12. Error bars show 2σ error. ~15 cm/ky, ~70 cm/ky, ~40 cm/ky are linear sedimentation rate for the Holocene, early deglaciation, the last glacial period, respectively.

2~4 mg of planktic foraminifera ***N. dutertrei*** were used for the AMS measurement.

AMS ^{14}C ages were converted to calendar ages by using calib. 6.0 with marine 09 and local reservoir correction of +29 yr.

Results

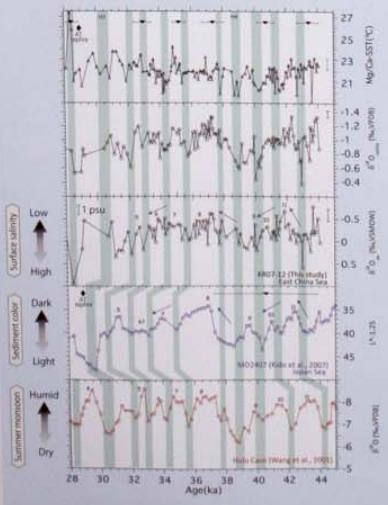

Fig. 7 (a) Mg/Ca-SST of G. ruber KR07-10 in the northern East China Sea (this study), (b) $\delta^{18}O$ of calcite G. ruber (this study), (c) $\delta^{18}O$ of seawater with global ice-volume correction by using a sea-level curve of Waelbroeck et al et al. [2002], (d) L* of MD2407 [Kido et al., 2007], (e) $\delta^{18}O$ of stalagmite record in Hulu Cave [Wang et al., 2001]. Triangles represent ^{14}C age controlling points with 2σ errors. Diamonds show the age controlling points by AT tephra (29 ka). Numbers in figures 1c, 1d, and 1e represent D-O cycle numbers.

Mg/Ca in fossil foraminiferal calcite

SST = ln (Mg/Ca/ 0.38)/0.089- (1) [Hatings et al., 2001]
SST: Sea surface temperature
※Planktic foraminifera "*G. ruber* "
①Dwelling: upper 30 m in water column
②Season: May to August (Xu et al., 2005)

Oxygen isotope ($\delta^{18}O$)

SST =14.9 - 4.8 ($\delta^{18}O_{calcite}$ - $\delta^{18}O_{sw}$)- (2) [Bemis et al., 1998]
$\delta^{18}O_{sw}$: Oxygen isotope of ambient seawater
※Locally, $\delta^{18}O$ is linearly related to sea surface salinity [Oba, 1998].
※Global ice volume effect was corrected by Waelbroeck et al., 2002)

Discussions

①. Approximately 1‰ amplitude of variations in surface salinity variations is equivalent to 5 psu in salinity, if the modern saliniy- $\delta^{18}O_{sw}$ relationship [Oba, 1998] is used.

②. From 44 to 38 ka, millennial-scale variations in $\delta^{18}O_{sw}$ in the northern East China Sea correlate well with those in L* in the Japan Sea, although the interstadial #10 and #11 are ~1 ky younger than those in Hulu Cave due to the error of the age models . Stadial #10 is recognized clearly in the East China Sea and in the Japan Sea, while that is not obvious in Hulu Cave.

1. Temperature

①. SST oscillates by ~3℃ during MIS3
②. Lower SST correspond to Heinrich events #4 and #3, and D-O stadial #5, 6, 7, 10, and 11. It suggests **teleconnection between the East China Sea and north Atlantic climate.**

2. Salinity ($\delta^{18}O_{sw}$)

①. $\delta^{18}O$ of seawater ($\delta^{18}O_{sw}$) oscillates by ~ 1‰ during MIS3.
②. Heavier $\delta^{18}O_{sw}$ corresponds to Heinrich events #4 and stadial #3, 5, 6, 7, 10, and 11.
③. **Temporal variation in $\delta^{18}O_{sw}$ agrees well with that of L* in the Japan Sea,** supporting that the nutrient-rich coastal water of the East China Sea entered to the Japan Sea and caused deposition of dark layers.

③. From 38 to 28 ka, interstadial #6 is obvious in $\delta^{18}O_{sw}$ in the East China Sea while that is not clear in L* of the Japan Sea sediments.

Conclusion

Our results support the idea that the intrusion of the East China Sea coatal water caused repeated deposition of dark layers in the Japan Sea on millennail-scale during MIS 3.

References

Acknowledgment

The travelling and accommodation fees are supported by GCOE of Department of Earth and Planetary Science, University of Tokyo.

Holocene flood frequency and redox-state evolution in meromictic Lake Cadagno (Swiss Alps)

ETH Eidgenössische Technische Hochschule Zürich Swiss Federal Institute of Technology Zurich

Sedimentology eawag

Stefanie B. Wirth[1], Adrian Gilli[1], Helge Niemann[2], Tais W. Dahl[3], Moritz F. Lehmann[2], Flavio S. Anselmetti[4]

[1] Geological Institute, ETH Zurich; [2]Department of Environmental Sciences, University of Basel; [3]Institute of Biology and NordCEE, University of Southern Denmark; [4]Department of Surface Waters, Eawag, Swiss Federal Institute of Aquatic Science and Technology

Introduction

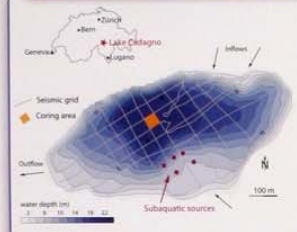

Figure 1: Bathymetric map of Lake Cadagno with seismic grid and coring area.

Lake Cadagno is a meromictic high-alpine lake situated in the Piora valley in the Southern Alps of Switzerland (1921 m asl, 0.26 km², max. water depth 21 m).

The inflow of salt-rich waters from subaquatic springs results in a permanent chemocline at 11 m, with anoxic bottom waters and a diverse anaerobic community of bacteria at and below the redox-transition zone. The modern redox conditions in Lake Cadagno are well studied, however, hardly anything is known about the paleoenvironmental conditions of the lake throughout the Holocene.

With this study we address the following questions:

- When did the chemocline form?
- Has it persisted since its formation?
- How frequent are flood events during the Holocene and do underfows affect the stability of the chemocline?

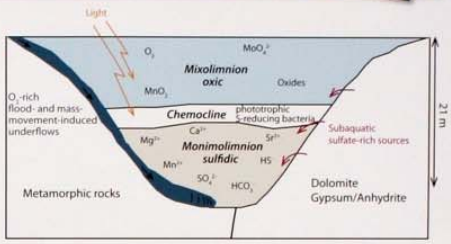

Figure 2: Sketch of present redox conditions and stratification in Lake Cadagno.

Formation of the chemocline

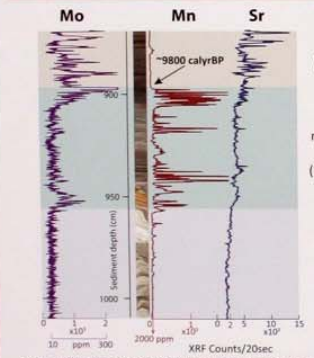

Figure 3: XRF core scanning data illustrating the formation of the chemocline.

The transition from oxic to anoxic conditions, including the formation of the chemocline, can be tracked in the XRF core scanning data.

- **oxic**: low Mo and Mn counts
- **manganiferrous**: high Mn counts, Mo counts begin to rise
- **sulfidic**: increase in Mo counts, decline in Mn
- **Sr**: possibly indicates the activation and the inflow of the subaquatic springs

The chemocline was fully established ~9800 cal yr BP. Before, the manganiferrous conditions persisted about 1000 years, providing a time frame for the chemocline formation.

Holocene flood record & continuing sulfidic conditions

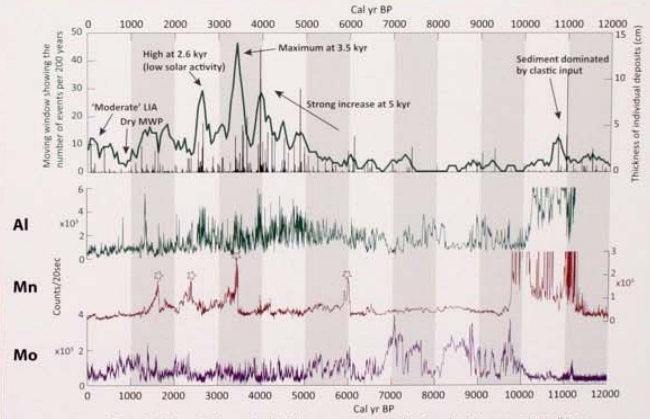

Figure 5: Holocene flood record and XRF data presenting detrital input and continuous anoxic conditions.

The Holocene **flood record** is characterised by a strong increase in flood frequency at 5 kyr and maximal flood activity between 2.5 and 4.5 kyr.

- **Al** as a detrital element reflects the clastic input delivered by the flood-induced underflows.

The **chemocline** and the **sulfidic conditions** have persisted throughout the Holocene.

- Moderate peaks of **Mn** (↔) during the Holocene indicate 'short-term oxygenation events' generated by mass-movements and intense flooding periods.
- Holocene **Mo** concentrations indicate persistent sulfidic conditions. However, periods of frequent flooding can reduce Mo burial by a factor 2.

Hypothesis for Mo and Mn behaviour during the three redox states

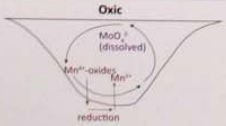

Mo occurs in its dissolved state, Mn-oxides are sedimented but partly reduced and Mn^{2+} is released from the sediment.

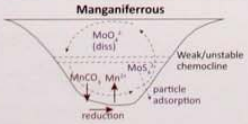

Intensified Mn-cycle due to more reducing conditions. Mo starts to be partially sulfidized and adsorbed to particles.

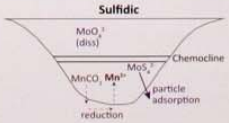

Mn mainly occurs in its reduced form Mn^{2+}. Mo burial by sulfidizaton and adsorption to particles is intensified.

What could have triggered the formation of the chemocline?

- Climate warming: warming of surface waters leads to stronger density gradient in the water column.
- Activation of subaquatic springs: the input of salt-rich water also leads to a stronger density gradient. This may as well be a signal of climate warming.

References

- Dahl et al. (2010) The behavior of molybdenum and its isotopes across the chemocline and in the sediments of sulfidic Lake Cadagno, Switzerland. Geoch. et Cosmoch. Acta, 74, 144-163.
- Del Don et al. (2001) The meromictic alpine Lake Cadagno: Orographical and biogeochemical description. Aquat. Sci., 63, 70-90.
- www.climategeology.ethz.ch/projects/floodalp
- www.eawag.ch/organisation/abteilungen/surf/schwerpunkte/project_overview/flood_alp/index_EN
- www.cadagno.ch